

## Research Paper

## A Novel Influence Function M-Estimator-Based for Active Noise Control

Seyed Amir HOSEINI SABZEVARI<sup>1)\*</sup>, Seyed Iman HOSSEINI SABZEVARI<sup>2)</sup><sup>(1)</sup> Department of Mechanical Engineering, University of Gonabad  
Gonabad, 9691957678, Iran

\*Corresponding Author e-mail: hoseini.sabzevari@gonabad.ac.ir

<sup>(2)</sup> Department of Electrical Engineering, Ferdowsi University of Mashhad  
Mashhad, 9177948974, Iran

(received February 4, 2020; accepted June 15, 2021)

M-estimators are widely used in active noise control (ANC) systems in order to update the adaptive FIR filter taps. ANC systems reduce the noise level by generating anti-noise signals. Up to now, the evaluation of M-estimators capabilities has shown that there exists a need for further improvements in this area. In this paper, a new improved M-estimator is proposed. The sensitivity of the proposed algorithm to the variations of its constant parameter is checked in feedforward control. The effectiveness of the algorithm in both types is proved by comparing it with previous studies. Simulation results show the steady performance and fast initial convergence of the proposed algorithm.

**Keywords:** active noise control; adaptive FIR; M-estimator; noise model.



Copyright © 2021 S.A. Hoseini Sabzevari, S.I. Hosseini Sabzevari  
This is an open-access article distributed under the terms of the Creative Commons Attribution-ShareAlike 4.0 International (CC BY-SA 4.0 <https://creativecommons.org/licenses/by-sa/4.0/>) which permits use, distribution, and reproduction in any medium, provided that the article is properly cited, the use is non-commercial, and no modifications or adaptations are made.

## 1. Introduction

Nowadays, acoustic noises become one of the most common and yet troublesome problems that humanity is dealing with. Because of the increasing application of industrial equipment, such as engines, gears, and compressors, people suffer from acoustic noises alongside mechanical vibration practically everywhere (KUO, MORGAN, 1999; NUNEZ, MIRANDA *et al.*, 2019). Based on the temporal feature of the acoustic noises, they can be categorized into two general groups, i.e. high-frequency and low-frequency acoustic noises. Passive noise control (PNC) methods have been used widely in order to compensate acoustic noises, for instance using enclosures to limit the acoustic noise of vacuum pumps or utilizing noise barriers to protect inhabitants of urban areas from roadway noise. Although there are various PNC methods for mitigating the noise level, these methods are bulky, costly, and are able to attenuate only high-frequency noises therefore they are ineffective at low frequencies (LEE *et al.*, 2010; DARVISH *et al.*, 2015; SABET *et al.*, 2018). In order to reduce low-frequency noises, active noise control (ANC) (NELSON, ELLIOTT, 1991; ELLIOTT, 2000; TAN, JIANG, 2015;

LU, ZHAO, 2017; SABZEVARI, MOAVENIAN, 2017) was proposed by (PAUL, 1936) in the early 20th century.

ANC is a wave control technique based on the superposition principle, in other words, the ANC system cancels noise around the target location by generating an anti-noise wave with the same amplitude but the opposite phase of the primary noise. Consequently, the transmitted acoustic wave combines with the primary noise, resulting in mitigation of primary noise (AKHTAR, MITSUHASHI, 2010; LI, CHEN, 2018; KHAN *et al.*, 2019). As can be seen in Fig. 1, a simple ANC system consists of two microphones, to pick up primary noise and the ambient noise at the focused area,

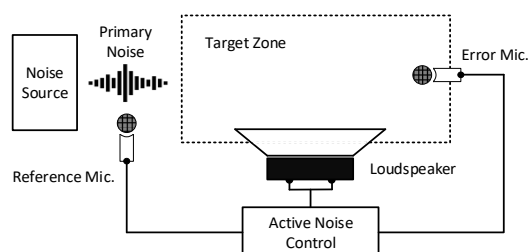


Fig. 1. Structure of an ANC system.

a loudspeaker for producing the anti-noise wave, and the control system.

In general, the control of ANC can be classified into two main groups, i.e. feedback methods and feedforward techniques. According to the type of primary noise, feedforward control can be further categorized into narrow-band and broad-band types (KUO, MORGAN, 1999). In contrast, in the feedback type, the ANC system does not use the primary noise measurements for mitigating the primary noises. Consequently, utilizing the feedback control method simplifies the control system and reduce the cost of the system. This method has been utilized by a wide range of headphone (ANG *et al.*, 2017; VU, CHEN, 2017).

The quality of the performance of the ANC system depends on the phase and amplitude of the generated anti-noise signal. As the recorded primary noise is subjected to a signal processing algorithm for analyzing, the characteristics of the generated anti-noise can be affected by the performance of the signal processing algorithm. The feature of the environment and characteristics of the noise are time-dependent inherently. Therefore, in order to overcome these fluctuations, almost all types of advanced ANC systems use adaptive algorithms to adjust ANC parameters (PATEL, GEORGE, 2015; BEHERA *et al.*, 2017). The most well-known adaptation approach used in ANC systems is based on filtered-x least mean square (FxLMS) algorithm due to its simplicity and robustness. However, in the impulsive environment, the transient outliers lead to transient fluctuation. These fluctuations could have adverse influences on the convergence and reduce the stability of the control system. In order to improve the performance of adaptive filters against outliers, M-estimators have been proposed in the literature (SEN, MORGAN, 1996; THANIGAI *et al.*, 2007). WU and QIU (2013) presented a new M-estimator algorithm subjected to impulse-like noise control. The proposed method shows better performance in comparison to the Hampel algorithm in Gaussian noises while it has a lower complexity. THANIGAI *et al.* (2007) proposed an M-estimator for enhancing the performance of the LMS algorithm. The presented method was implemented in the infant incubator and the simulation results indicate rather improved performance with respect to the simple LMS. However, the simu-

lations were performed only in a few scenarios. ERTAŞ *et al.* (2017) proposed a novel Li-type M-estimator. Although the proposed algorithm shows robust performance against outliers and multicollinearity, the superiority of the proposed method limited to scenarios with several assumptions and specific conditions. SUHAIL *et al.* (2019) proposed a ridge M-estimator based on a quantile value. The performance of the presented method compared with fair amount of different M-estimators and the simulations result showed a satisfactory performance.

In this paper, an improved M-estimator for ANC of impulsive noises is proposed. The presented method shows a better performance in comparison with the other methods presented in previous studies. In addition, not only the proposed algorithm shows robustness along with convenient stability but also achieves convergence more quickly than other methods.

The rest of the paper is laid out as follows: in Sec. 2 the proposed improved M-estimator algorithm is derived. The simulations that confirm the effectiveness of the proposed algorithm are described in Sec. 3, and the paper is concluded in Sec. 4.

## 2. The system structure

The block diagram of a feedforward ANC system is illustrated in Fig. 2 where  $x(n)$  and  $y(n)$  represent the primary noise and anti-noise signals, respectively. As can be seen, the structure of the system consists of two main paths. The  $P(z)$  is equivalent to the plant response which is basically dynamic and has the unknown characteristics. The secondary path which produces the corresponding response from the ANC algorithm and the loudspeaker contains a FIR filter called  $S(z)$ . The  $S(z)$  function is a finite impulse response (FIR) filter used to produce the acoustic response to the reference microphone signals. Because the primary noise is sampled only in feedforward systems, this path is not available in the structure of feedback type systems. It is important to notice that although the responses of the two paths are subtracted as shown in Fig. 2, in fact, the acoustic responses of the two paths are summed in the target zone. The use of subtraction is only needed because of building consistency with the common control structures.

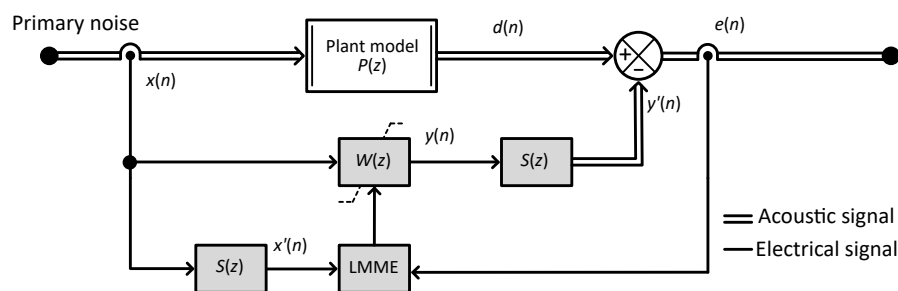


Fig. 2. Feedforward block diagrams of FxLMME based ANC system.

The  $W(z)$  function is an adaptive filter meant to minimize the error signal, i.e. the  $e(n)$  signal. The coefficients of the  $W(z)$  function are adjusted by using an algorithm called the Least Mean M-estimator (LMME). The LMME algorithm attempts to minimize a cost function represented as  $\sum_i \rho(e_i)$ , where  $\rho(x)$  is a symmetric positive definite function that has a minimum at zero (WUM, QIU, 2013). The most common form of  $\rho(x)$  is  $x^2/2$  and it is known as the Least Mean Square (LMS). The cost function of the LMME based ANC system is given in Eq. (1) (SEN, MORGAN, 1996; WU, QIU, 2013)

$$J_{ME} = E[\rho(e(n))] \approx \rho(e(n)). \tag{1}$$

The parameters of the adaptive filter,  $W(z)$ , are updated according to Eq. (2) (SEN, MORGAN, 1996)

$$\begin{aligned} W(n+1) &= W(n) - \mu \nabla J_{ME} \\ &= W(n) + \mu \phi(e(n)) [\widehat{s}(n) * x(n)], \tag{2} \end{aligned}$$

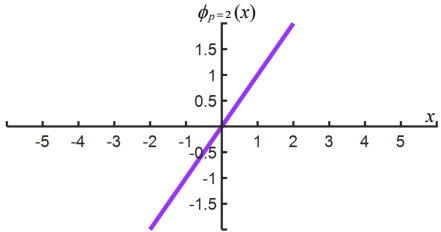
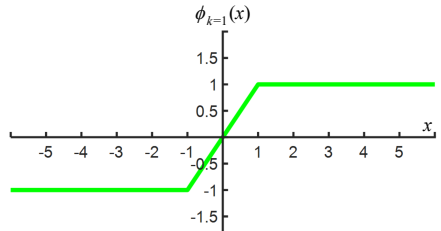
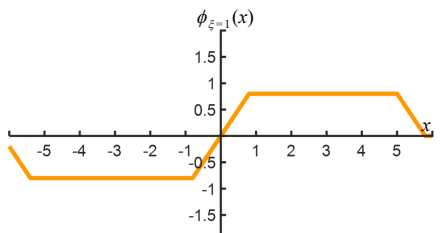
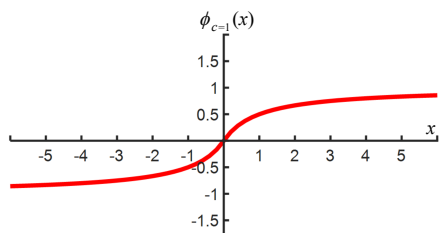
where  $\mu$  is the step size demonstrating the convergence. The maximum value of  $\mu$  was derived by (KUO, MORGAN, 1999). The function  $\phi(e(n))$  is the derivative of the function  $\rho(e(n))$  which is called the influence function. Here “\*” stands for the linear convolution and the result of  $\widehat{s}(n) * x(n)$  is the filter’s reference signal.

2.1. Influence function

If LMS is not used, there will be instability in the results when the data contain outliers samples (WU, QIU, 2013). The influence function for LMS is  $\phi(x) = \frac{d\rho(x)}{dx} = x$ . Therefore, the results would increase unrestrictedly which leads to instability as the input of the function increases. To overcome this deficiency, various forms of  $\rho(x)$  were introduced.

In most of the existing methods,  $\rho(x)$  is determined to enforce a bounded influence function. Table 1 demonstrates some of the most commonly used functions in which  $p, \iota, \xi, \alpha,$  and  $\beta$  are the arbitrary para-

Table 1. Equivalent M-Estimators and their schematic influence function.

Name	$\rho(x)$	Influence function
$L_p$	$\frac{ X ^p}{p}$	
Huber	$\begin{cases} \frac{X^2}{2} & \text{for }  X  \leq K \\ K \left(  X  - \frac{K}{2} \right) & \text{for }  X  > K \end{cases}$	
Hampel	$\begin{cases} \frac{X^2}{2} & \text{for }  X  \leq \xi \\ \xi \left(  X  - \frac{\xi}{2} \right) & \text{for } \xi <  X  \leq \alpha \\ \frac{\xi}{2}(\alpha + \beta) - \frac{\xi^2}{2} + \frac{\xi}{2} \frac{( X  - \beta)^2}{(\alpha - \beta)} & \text{for } \alpha <  X  \leq \beta \\ \frac{\xi}{2}(\alpha + \beta) - \frac{\xi^2}{2} & \text{for }  X  > \beta \end{cases}$	
Fair	$C^2 \left[ \frac{ X }{C} - \log \left( 1 + \frac{ X }{C} \right) \right]$	

meters. The mentioned influence functions show different performance according to the value of the  $p$ . Therefore, in order to be able to evaluate the performance of selected influence functions properly, the value of  $L_p$  when  $p = 2$  as in (WU, QIU, 2013), is assumed as the fundamental performance. For example, when  $p = 2$ ,  $L_p$  gives  $\rho(x) = 0.5 \cdot |x|^2$  and the influence function is equal to  $\phi(x) = x$ . The mentioned restriction of LMS can also be expressed according to Table 1. Considering the discussions had by Lifu Wu and Xiaojun Qiu (KUO, MORGAN, 1999) regarding the functions shown in Table 1, one can notice that although  $L_p$  is a direct algorithm, it causes instability by not implementing a limit on the influence function value.

The Huber function is a combination of two values of  $L_p$ , when  $p = 1$  and  $p = 2$ . Although the simulation results of the Huber function show better stability than fundamental  $L_p$ , its abrupt limitations may cause instability. On the other hand, the Hampel function which resembles a combination of the Huber,  $L_p$ , and an incipient decrease in limitation of the influence function value, requires a considerable computational effort. The Fair function bounds  $\phi(x)$  take advantage of both  $L_1$  and  $L_2$  in order not only to reduce the effect of large errors but also remain convex (THANIGAI *et al.*, 2007). These functions ( $\rho(x)$ ) and their influence functions using arbitrary constant parameters are illustrated in Fig. 3.

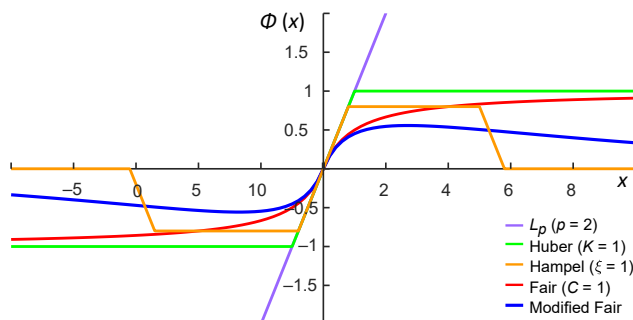


Fig. 3. Influence function of Fair, Modified Fair, Huber, Hampel, and  $L_2$  algorithms.

### 2.2. The proposed influence function

The Fair function is a modified form of the Huber function calculated by changing the hard limitations

into a smooth one. However, in this paper an influence function will be proposed which takes advantage of both the Fair and the Hampel functions by changing the hard limitations into a smooth function. The proposed influence function is called the Modified Fair and is presented in Fig. 4. This figure indicates the differences between the Fair and the proposed Modified Fair function.

A value between 1 and 2 is recommended for the parameter  $C$  in the Fair algorithm (WU, QIU, 2013). The value of  $C$  is chosen to be equal to one here. According to the value of input errors, the behaviour of the influence function of the Modified Fair algorithm can be categorized into three parts, i.e. Part-1 – small errors, Part-2 – moderate errors, and Part-3 – large errors. When the input error is limited to small values, the Modified Fair algorithm acts like  $L_2$ . If the value of errors increases, the performance of the Modified Fair algorithm adapts accordingly and benefits from the advantage of the Fair algorithm. By further incensement of the input errors, the Modified Fair method covers the advantages of the Hampel function.

In the Modified Fair algorithm,  $\lambda$  is a constant parameter related to the average absolute amplitude of error (AE)

$$\lambda = C \times AE, \tag{3}$$

where  $C$  is a constant number, and  $AE$  is represented by Eq. (4):

$$AE(n) = \frac{1}{M} \sum_{i=0}^{M-1} |e(n-i)|. \tag{4}$$

In Eq. (4), the parameter  $M$  is a moving window with the length  $M = 350$ .

### 2.3. Noise model

There are two famous noise models which use probability density functions:

- Gaussian Mixture Model (GMM)

$$f(x) = (1 - \varepsilon)G(x) + \varepsilon I(x), \tag{5}$$

where  $\varepsilon$  is a small constant number; and  $G(x)$  and  $I(x)$  are Gaussian probability functions. The variance of  $I(x)$  should be greatly larger than  $G(x)$  (WU, QIU, 2013).

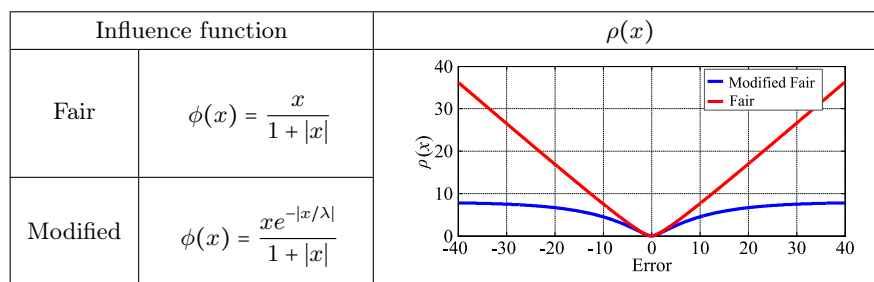


Fig. 4. Comparison of Fair and Modified Fair algorithm.

- Additive Impulsive Noise (AIN)

$$g(x) = G(x) + \phi(x), \quad (6)$$

where  $G(x)$  is the same as before and  $\phi(x)$  is a non-Gaussian distribution which is often a standard symmetric  $\alpha$  stable distribution (standard  $S\alpha S$ ) where  $S\alpha S$  is represented by:

$$S\alpha S(t) = e^{-\gamma|t|^\alpha}, \quad (7)$$

where  $\alpha$  is a characteristics exponent ( $0 < \alpha < 2$ ) and  $\gamma$  is a positive number known as dispersion which is equal to one in the standard  $S\alpha S$ . For  $\alpha = 2$  the distribution is a Gaussian and for  $\alpha = 1$  it is a Cauchy distribution (AKHTAR, MITSUHASHI, 2010). In this paper, both models are used.

### 3. Simulation results

In this section, the effectiveness of the Modified Fair algorithm is discussed and compared with the Fair Algorithm. In addition, the ANC models are generated to verify the behaviour of the proposed algorithm by carrying out in four steps. At first, the primary noise is modelled. Then, the performance comparisons are designed and in the next step, the constant parameter is selected. Finally, the sensitivity test and noise simulation are utilized.

#### 3.1. Performance comparison

In order to compare the performance of different LMME algorithms, most studies have used average (arithmetic mean) noise reduction (ANR/AMR) defined as:

$$ANR(n) = 20 \log_{10} \frac{A_d(n)}{A_e(n)}, \quad (8)$$

$$A_d(n) = \nu A_d(n-1) + (1-\nu)|e(n)|, \quad (9)$$

$$A_e(n) = \nu A_e(n-1) + (1-\nu)|d(n)|,$$

where  $\nu$  is a constant number  $0.9 < \nu < 1$  called forgetting factor, signals  $d$  and  $e$  are the disturbance and error, respectively as illustrated in Fig. 2. Each ANR curve is obtained as shown in (WU, QIU, 2013) by calculating the average of 100 ANR curves generated using 100 different noise models.

#### 3.2. Parameter values

All the constant parameters are chosen to be the same as in (WU, QIU, 2013) in order to make the results comparable with each other.  $S(z)$ ,  $P(z)$ , and  $W(z)$  are modelled by FIR filters with 250, 800, and 350 taps, respectively. The  $\varepsilon$  in GMM is chosen to be 0.05 and the forgetting factor in ANR is  $\nu = 0.999$ .

#### 3.3. The sensitivity of the Modified Fair Algorithm

The constant parameter  $C$  in the Modified Fair algorithm, as shown in Eq. (3), may have a large domain of values. In order to choose a specific value, the sensitivity of the algorithm was analysed by using different values of  $C$ . The feedforward model was generated and the reference noise signal was modelled by both GMM and AIN ( $\alpha = 1.1$ ). The parameter  $C$  in Eq. (3) was chosen to be 1, 1.5, 5, 10, and 20, respectively. The results are illustrated in Fig. 5.

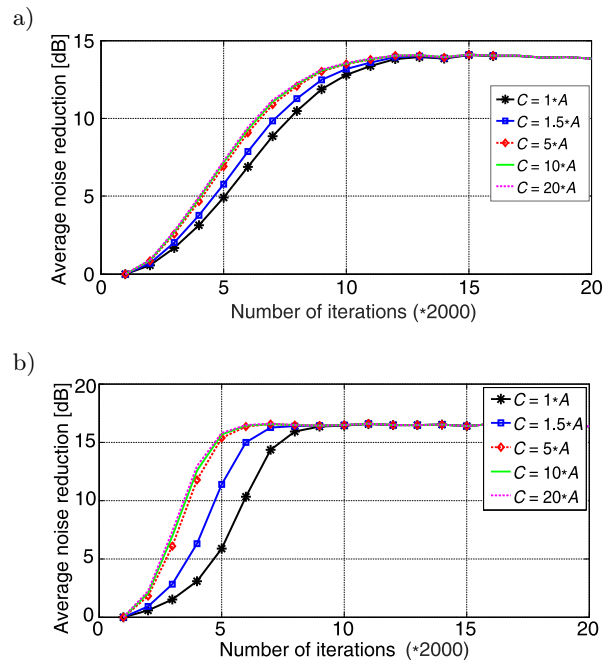


Fig. 5. The average noise reduction of Modified Fair algorithm in “feedforward model” associated with references noise signal modelled by: a) GMM and b) AIN.

According to Fig. 5, the maximum difference between the curves in the feedforward model with GMM and AIN is around 2 and 9 dB, respectively. In both cases, the differences decrease rapidly by increasing the value of  $C$ ; and the maximum difference in the curves with  $C > 4$  was less than 0.5 dB.

Therefore, the Modified Fair algorithm is insensitive to the choice of parameter  $C$  when  $C > 4$ . Hence, the optimum value of parameter  $C$  should be greater than 4. In this study, the parameter  $C$  is set to be  $C = 5$ .

#### 3.4. Simulated noise

In this section, the performance of the Fair and the proposed Modified Fair algorithms are compared in the feedforward model. In each model, GMM and AIN are used to generate the reference noise signals with three different conditions as shown in Table 2. For GMM, the distributions of  $G(x)$  and  $I(x)$  are chosen to be normal with average equal to zero. In both models, the

Table 2. Different conditions for AIN and GMM models.

Noise model	AIN	GMM
Case-1	$\alpha = 1.6$	$\frac{\text{variance } I(x)}{\text{variance } G(x)} = 10$
Case-2	$\alpha = 1.4$	$\frac{\text{variance } I(x)}{\text{variance } G(x)} = 100$
Case-3	$\alpha = 1.2$	$\frac{\text{variance } I(x)}{\text{variance } G(x)} = 1000$

impulsiveness of generating noise is increasing as the case number is increased (Case-3 > Case-2 > Case-1). Figures 6 and 7 illustrate the performance of the Fair and the Modified Fair algorithms in several different scenarios.

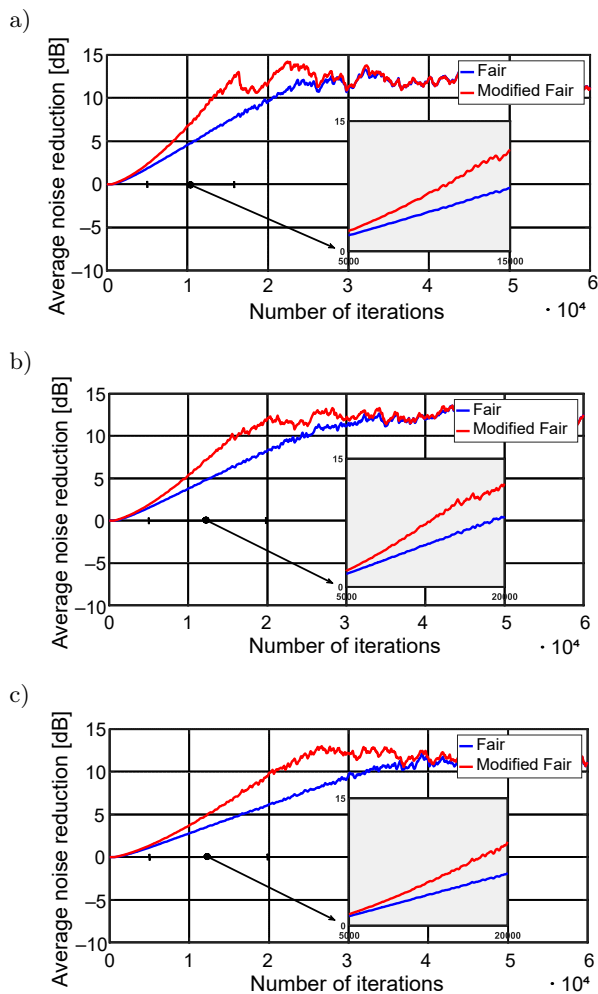


Fig. 6. Comparison of Fair and Modified Fair algorithms in feedforward type:

- a) GMM Case-1 ( $\mu_{\text{Fair}} = 1 \cdot 10^{-4}$ ,  $\mu_{\text{Modified}} = 1 \cdot 10^{-4}$ ),
- b) GMM Case-2 ( $\mu_{\text{Fair}} = 1 \cdot 10^{-5}$ ,  $\mu_{\text{Modified}} = 2 \cdot 10^{-5}$ ),
- c) GMM Case-3 ( $\mu_{\text{Fair}} = 1 \cdot 10^{-6}$ ,  $\mu_{\text{Modified}} = 2 \cdot 10^{-6}$ ).

Figures 6 and 7 show the performance of the algorithms with GMM and AIN noise models of feed-

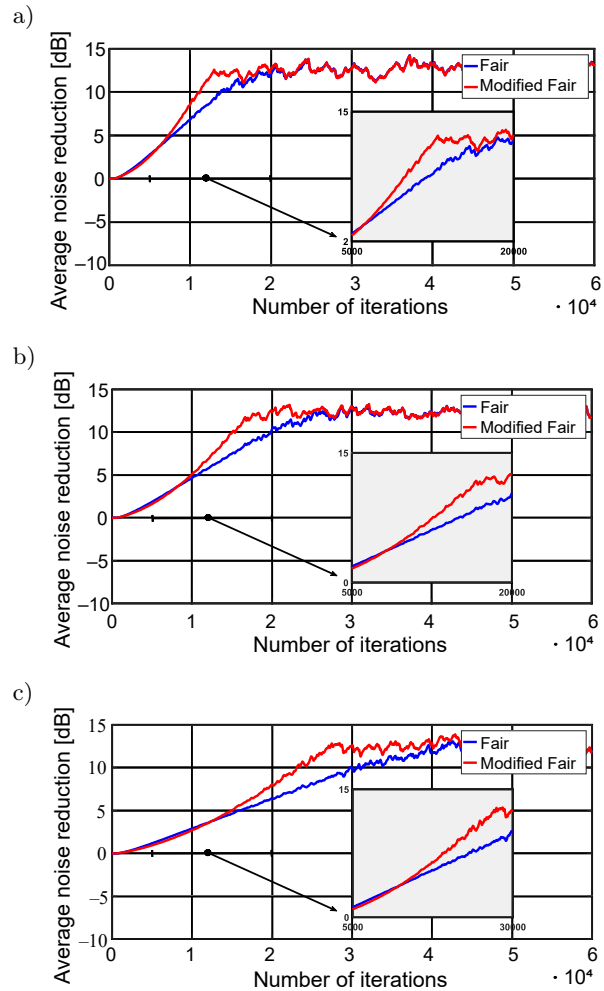


Fig. 7. Comparison of Fair and Modified Fair algorithms in feedforward type:

- a) AIN Case-1 ( $\mu_{\text{Fair}} = 1 \cdot 10^{-7}$ ,  $\mu_{\text{Modified}} = 1 \cdot 10^{-7}$ ),
- b) AIN Case-2 ( $\mu_{\text{Fair}} = 1 \cdot 10^{-8}$ ,  $\mu_{\text{Modified}} = 2 \cdot 10^{-8}$ ),
- c) AIN Case-3 ( $\mu_{\text{Fair}} = 2 \cdot 10^{-9}$ ,  $\mu_{\text{Modified}} = 3 \cdot 10^{-9}$ ).

forward type. In the GMM cases, the maximum differences between the algorithms are decreasing by increasing the impulsiveness of noise, whereas they are increasing in the AIN cases. When errors are small, the performance of the two algorithms is exactly similar to each other. So, the differences between them after convergence can be neglected while those before convergence cannot.

However, the Modified Fair model shows a faster initial convergence than the Fair model in the case of both noise models in all scenarios as demonstrated in Table 3. The proposed Modified Fair algorithm shows the best performance improvement in its initial convergence rate in case 3 with a reduction of the number of iterations to reach 90% of its final value to 11366 and 9156 in the GMM and AIN cases, respectively. The residual error signal,  $e(n)$ , of the Fair and the proposed Modified Fair algorithms for both noise models are illustrated in Fig. 8.

Table 3. Comparison of the number of iterations for the Fair and the Modified Fair models to converge to 90% of their final values.

Noise Model	GMM			AIN		
	Case-1	Case-2	Case-3	Case-1	Case-2	Case-3
Fair	22491	26134	33058	15848	24025	34481
Modified Fair	14575	18113	21692	12084	16922	25325
The reduction in the number of iterations	7916	8021	11366	3764	7103	9156

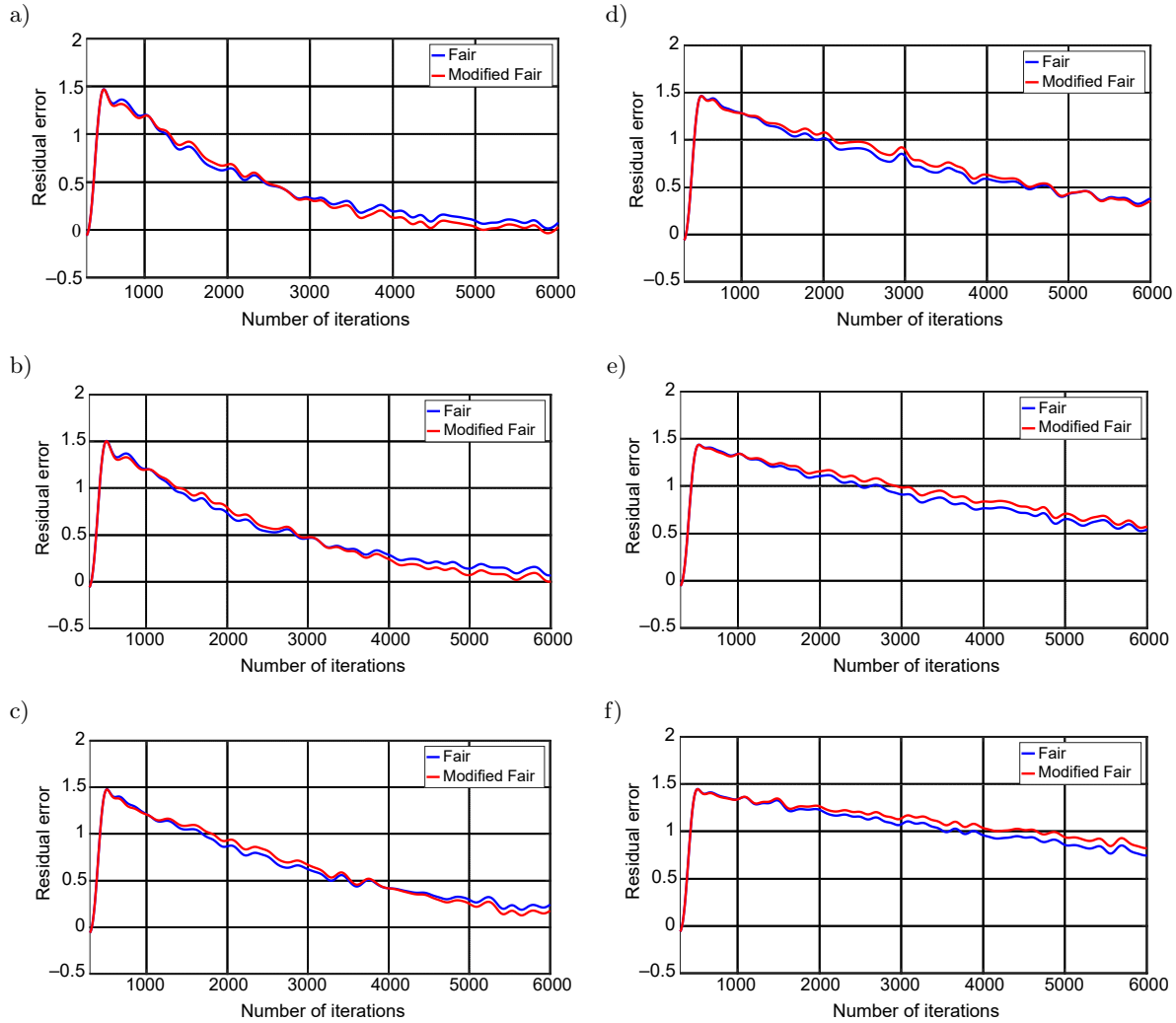


Fig. 8. Residual error of Fair and Modified Fair algorithm: a) GMM Case-1, b) GMM Case-2, c) GMM Case-3, d) AIN Case-1, e) AIN Case-2, f) AIN Case-3.

From the simulation results presented in Figs 4–7 and Tables 2 and 3, we can conclude that:

- The proposed Modified Fair algorithm has a faster initial convergence compared with the Fair algorithm in all three scenarios. Quantitative data revealed that the proposed Modified Fair algorithm is superior, e.g. it is able to yield a fast convergence in impulsiveness noises.
- The Modified Fair algorithm has a similar residual noise performance to the Fair algorithm. However,

it has a faster initial convergence than the Fair algorithm without losing stability.

#### 4. Conclusion

The new modified M-estimator proposed in this paper demonstrates considerable improvements regarding its influence function capabilities. It was shown that the sensitivity of the proposed algorithm to its constant parameter is negligible. Conducted computer

simulations indicate that the proposed modified M-estimator has a fast initial convergence rate, steady performance, and proper robustness. The results are compared with recently published works while generating primary noise with Gaussian and Non-Gaussian models. In the future, it would be interesting to perform a real-time experiment by developing a prototype system and comparing the proposed method with other existing modified M-estimator algorithms such as the one considered in (SUN *et al.*, 2015).

## References

- AKHTAR M.T., MITSUHASHI W. (2010), A modified normalized FxLMS algorithm for active control of impulsive noise, *Proceedings of 18th European Signal Processing Conference (EUSIPCO)*, IEEE, pp. 1–5, Aalborg.
- ANG L.Y.L., KOH Y.K., LEE H.P. (2017), The performance of active noise-canceling headphones in different noise environments, *Applied Acoustics*, **122**: 16–22, doi: 10.1016/j.apacoust.2017.02.005.
- BEHERA S. K., DAS D.P., SUBUDHI B. (2017), Adaptive nonlinear active noise control algorithm for active headrest with moving error microphones, *Applied Acoustics*, **123**: 9–19, doi: 10.1016/j.apacoust.2017.03.002.
- DARVISH M., FRANK S., PASCHEREIT C.O. (2015), Numerical and experimental study on the tonal noise generation of a radial fan, *Journal of Turbomachinery*, **137**(10): 101005, doi: 10.1115/1.4030498.
- ELLIOTT S. (2001), *Signal Processing for Active Control*, Academic Press, Elsevier.
- ERTAŞ H., KAÇIRANLAR S., GÜLER H. (2017), Robust Liu-type estimator for regression based on M-estimator, *Communications in Statistics-Simulation and Computation*, **46**(5): 3907–3932, doi: 10.1080/03610918.2015.1045077.
- KHAN W.U., YE Z., ALTAF F., CHAUDHARY N.I., RAJA M.A.Z. (2019), A novel application of fireworks heuristic paradigms for reliable treatment of nonlinear active noise control, *Applied Acoustics*, **146**: 246–260, doi: 10.1016/j.apacoust.2018.11.024.
- KUO S.M., MORGAN D.R. (1999), Active noise control: a tutorial review, *Proceedings of the IEEE*, **87**(6): 943–973, doi: 10.1109/5.763310.
- LEE J.W., LEE J.C., PANDEY J., AHN S.H., KANG Y.J. (2010), Mechanical properties and sound insulation effect of ABS/carbon-black composites, *Journal of Composite Materials*, **44**(14): 1701–1716, doi: 10.1177/0021998309357673.
- LI J., CHEN W. (2018), Singular boundary method based on time-dependent fundamental solutions for active noise control, *Numerical Methods for Partial Differential Equations*, **34**(4): 1401–1421, doi: 10.1002/num.22263.
- LU L., ZHAO H. (2017), Active impulsive noise control using maximum correntropy with adaptive kernel size, *Mechanical Systems and Signal Processing*, **87**(part A) 180–191, doi: 10.1016/j.ymsp.2016.10.020.
- NELSON P.A., ELLIOTT S.J. (1991), *Active Control of Sound*, Academic Press, Elsevier.
- NUNEZ I.J., MIRANDA J.G., DUARTE M.V. (2019), Active noise control in acoustic shutters, *Applied Acoustics*, **152**: 41–46, doi: 10.1016/j.apacoust.2019.03.024.
- PATEL V., GEORGE N.V. (2015), Nonlinear active noise control using spline adaptive filters, *Applied Acoustics*, **93**: 38–43, doi: 10.1016/j.apacoust.2015.01.009.
- PAUL L. (1934), Process of silencing sound oscillations, Google patents.
- SABET S.M., KESHAVARZ R., OHADI A. (2018), Sound isolation properties of polycarbonate/clay and polycarbonate/silica nanocomposites, *Iranian Polymer Journal*, **27**(1): 57–66, doi: 10.1007/s13726-017-0585-2.
- SABZEVARI S.A.H., MOAVENIAN M. (2017), Application of reinforcement learning for active noise control, *Turkish Journal of Electrical Engineering & Computer Sciences*, **25**(4): 2606–2613.
- SEN K.M., MORGAN D.R. (1996), *Active Noise Control Systems: Algorithms and DSP Implementations*, John Wiley and Sons.
- SUHAIL M., CHAND S., KIBRIA B.G. (2019), Quantile-based robust ridge m-estimator for linear regression model in presence of multicollinearity and outliers, *Communications in Statistics-Simulation and Computation*, 1–13, doi: 10.1080/03610918.2019.1621339.
- SUN G., LI M., LIM T.C. (2015), Enhanced filtered-x least mean M-estimate algorithm for active impulsive noise control, *Applied Acoustics*, **90**: 31–41, doi: 10.1016/j.apacoust.2014.10.012.
- TAN L., JIANG J. (2015), Active control of impulsive noise using a nonlinear companding function, *Mechanical Systems and Signal Processing*, **58**: 29–40, doi: 10.1016/j.ymsp.2015.01.010.
- THANIGAI P., KUO S.M., YENDURI R. (2007), Nonlinear active noise control for infant incubators in neonatal intensive care units, *Proceedings of 2007 IEEE International Conference on Acoustics, Speech and Signal Processing (ICASSP)*, IEEE, pp. 1–109, Honolulu, doi: 10.1109/ICASSP.2007.366628.
- VU H.-S., CHEN K.H. (2017), A high-performance feedback FxLMS active noise cancellation VLSI circuit design for in-ear headphones, *Circuits, Systems and Signal Processing*, **36**(7): 2767–2785, doi: 10.1007/s00034-016-0436-y.
- WU L., QIU X. (2013), An M-estimator based algorithm for active impulse-like noise control, *Applied Acoustics*, **74**(3): 407–412, doi: 10.1016/j.apacoust.2012.06.019.